

## Variability of the Denmark Strait overflow: Moored time series from 1996–2011

Kerstin Jochumsen,<sup>1</sup> Detlef Quadfasel,<sup>1</sup> Heðinn Valdimarsson,<sup>2</sup> and Steingrímur Jónsson<sup>2,3</sup>

Received 1 June 2012; revised 11 October 2012; accepted 16 October 2012; published 7 December 2012.

[1] The Denmark Strait overflow provides about half of the total dense water overflow from the Nordic Seas into the North Atlantic Ocean. The velocity of the overflow has been monitored in the Strait with two moored Acoustic Doppler Current Profilers since 1996 with several interruptions due to mooring losses or instrument failure. So far, overflow transports were only calculated when data from both moorings were available. In this work, we introduce a linear model to fill gaps in the time series when data from only one instrument is available. The mean overflow transport is 3.4 Sv and exhibits a variance of 2.0 Sv<sup>2</sup>. No significant trend was detected in the time series. The highest variability in the transport is associated with the passage of mesoscale eddies with time scales of 2–10 days (associated with a variance of 1.5 Sv<sup>2</sup>). Seasonal variability is weak and explains less than 5% of the variance in all time series, which is in contrast to the strong seasonal cycle found in high resolution model simulations. Interannual variability is on the order of 10% of the mean. A relation to atmospheric forcing such as the local wind stress curl, as well as to larger scale phenomena, e.g. the North Atlantic Oscillation, is not detected. Since 2005 data from moored temperature, conductivity and pressure recorders have been available as well, monitoring the hydrographic variability at the bottom of Denmark Strait. In recent years the temperature time series of the Denmark Strait overflow revealed a cooling, while the salinity stayed nearly constant.

**Citation:** Jochumsen, K., D. Quadfasel, H. Valdimarsson, and S. Jónsson (2012), Variability of the Denmark Strait overflow: Moored time series from 1996–2011, *J. Geophys. Res.*, 117, C12003, doi:10.1029/2012JC008244.

### 1. Introduction

[2] Denmark Strait is the pathway for about half of the dense water overflows from the Nordic Seas to the North Atlantic. It is thus one of the major sources of North Atlantic Deep Water [Dickson and Brown, 1994], the main water mass forming the lower limb of the Atlantic Meridional Overturning Circulation. The Strait has a sill depth of 640 m and is a wide passage (broader than the deformation radius), where the inflow and outflow are separated horizontally: Export of Polar Water occurs within the East Greenland Current (EGC) over the Greenland slope and shelf, while Atlantic inflow is found close to Iceland. The outflowing EGC is cold and fresh, while the northeastward Irminger Current (IC) brings warm and saline water into the Nordic Seas (Figure 1). Although the warm inflow is a persistent feature, it accounts for only about 10% of the total volume inflow to the Nordic Seas [Jónsson and Valdimarsson, 2012]. However, warm/cold surface temperatures

do not always coincide with northward/southward flow, indicating recirculations of both EGC and IC waters.

[3] A snapshot of the potential temperature distribution on a section along the sill of Denmark Strait is illustrated in Figure 2a. The IC waters are easily identified by the high temperatures, exceeding 6°C above 400 m depth on the Icelandic side of the strait, where also the strongest northeastward flow is apparent (Figure 2b). On the Greenland side of the section water temperatures are below 2°C, and the currents are weak. Swift southwestward currents are found in the whole water column over the deepest location. The overflow water, defined as  $\sigma_\theta > 27.8 \text{ kg m}^{-3}$ , fills the deep part of the section and shows a pronounced current core with velocities of up to  $-100 \text{ cm/s}$ . Overflow water is typically found at depths larger than 300 m; close to the sill it occupies an approx. 250 m thick layer in Denmark Strait [Macrandner et al., 2005]. A detachment of IC water is visible in the temperature distribution, but no strong currents are associated with this feature. Such lenses of warmer Atlantic Water were found to occur occasionally on the Greenland side of the section [Rudels et al., 2002]. On similar sections taken during other cruises, the IC was found to reach even into the deepest part of the section, thus restricting the overflow onto the Greenland slope of the strait.

[4] Several water masses contribute to the Denmark Strait overflow, but in a simple approach, these waters can be sorted into two classes [Våge et al., 2011]: “Atlantic origin”

<sup>1</sup>Institut für Meereskunde, Universität Hamburg, Hamburg, Germany.

<sup>2</sup>Marine Research Institute, Reykjavik, Iceland.

<sup>3</sup>School of Business and Science, University of Akureyri, Akureyri, Iceland.

Corresponding author: K. Jochumsen, Institut für Meereskunde, Universität Hamburg, Bundesstr. 53, DE-20146 Hamburg, Germany. (kerstin.jochumsen@zmaw.de)

©2012. American Geophysical Union. All Rights Reserved.  
0148-0227/12/2012JC008244

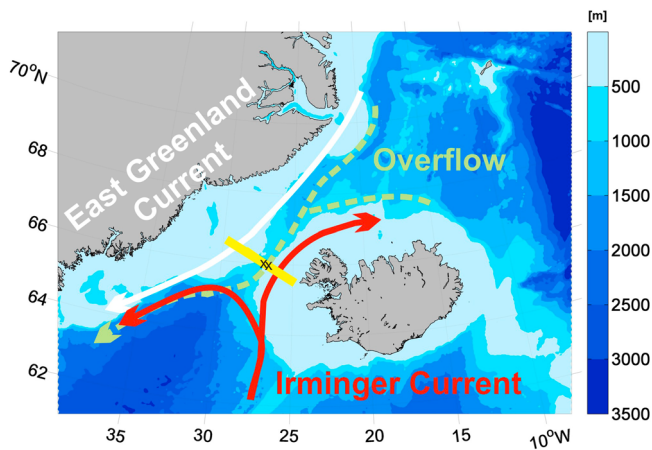


**Figure 1.** Topography of the Denmark Strait region, with schematic currents. Shelf regions shallower than 500 m are shaded in light blue colors. The location of the sill section depicted in Figure 2 at the shallowest region of Denmark Strait is indicated by the yellow line, with black crosses at the mooring positions.

waters, formed of Recirculated and Arctic Atlantic Water, and “Arctic origin” waters, summarizing e.g. Arctic Ocean Deep Water, upper Polar Deep Water, Greenland Sea Arctic Intermediate Water and Iceland Sea Arctic Intermediate Water. A multivariate analysis quantified the Atlantic source water supply to be between 30% and 50% of the overflow waters [Tanhua *et al.*, 2005]. For the densest layer of the overflow

with  $\sigma_\theta > 28.04 \text{ kg m}^{-3}$  the Arctic sources clearly dominate [Olsson *et al.*, 2005]. Nevertheless, the Arctic waters can reach the Denmark Strait sill on different pathways, either within the EGC or via detours through the Nordic Seas, where locally formed water masses are entrained. Våge *et al.* [2011] concluded that the densest overflow water is brought to Denmark Strait by the North Icelandic Jet, which supplies up to 50% of the overflow transport.

[5] Single and/or synoptic transport estimates by Worthington [1969], Ross [1984] and Garton *et al.* [2001] show the Denmark Strait overflow to be close to 3 Sv. A continuous monitoring of the overflow at the sill of Denmark Strait was initiated in 1996 using moored Acoustic Doppler Current Profilers (ADCPs). Mooring work in the strait is problematic because of intense fishing activities and several instruments were lost. The goal of maintaining persistent ADCP measurements at two locations was only reached during eight years since 1996. Nevertheless, data from five additional years with one operating instrument (at DS 1, cf. Figures 1 and 2) exist. The results of the measurements in the period 1999 to 2003 are presented in Macrander *et al.* [2005]. The authors found a significant decrease in the transport of the Denmark Strait overflow, and a warming of the near bottom layer. The annual transport of the overflow varied between 3.7 Sv and 3.1 Sv during their mooring period.

[6] Other long term observations of the overflow transport and properties are based on downstream mooring arrays [e.g., Dickson and Brown, 1994; Dickson *et al.*, 2008; Hall *et al.*, 2011], giving mean transport values of  $4.0 \pm 0.4 \text{ Sv}$  for density anomalies above  $\sigma_\theta = 27.85 \text{ kg m}^{-3}$ . These observations are focused on the overflow plume in the

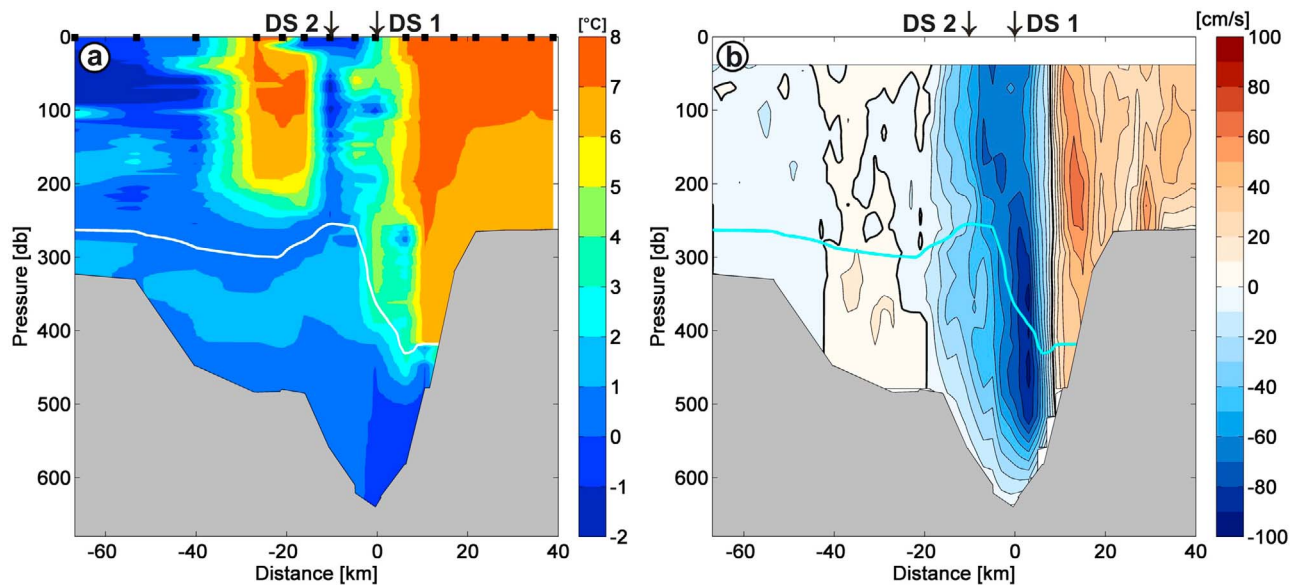


**Figure 2.** (a) Snapshot of potential temperature from CTD stations in July 2010 along the sill of Denmark Strait (interpolated between stations and extrapolated to the bottom); (b) Corresponding snapshot of de-tided cross-section velocity from the shipboard ADCP, interpolated to the bottom where the velocity was set to zero. Negative velocities are toward the south-southwest (blue), while positive velocities are north-northeastward (red). The isopycnal bordering the overflow is shown in white/cyan ( $\sigma_\theta = 27.8 \text{ kg m}^{-3}$ ). The x-axes give the distance from the deepest point on the sill of Denmark Strait, negative distances are towards the northwest (Greenland) and positive towards the southeast (Iceland). Black squares at the top of Figure 2a mark the positions where CTD stations were taken. The locations of the moorings DS 1 and DS 2 are pointed out by the black arrows.

Irminger Basin, which descends from Denmark Strait to 2500–3000 m depth near Cape Farewell [van Aken and de Jong, 2012]. However, some portion of the dense overflow water remains on the shelf and forms the East Greenland Spill Jet [e.g., Brearley *et al.*, 2012]. Cascades of dense shelf water were found to mix into the overflow plume in the northern Irminger Sea [Falina *et al.*, 2012]. These intermittent processes are sparsely observed and not captured by the traditional mooring arrays. Both the rapid descent of the overflow and the spill jet cascades induce entrainment of ambient waters, which adds to the overall transport, especially within the first 200 km from the sill [Voet and Quadfasel, 2010]. Therefore, measurements of the overflow directly at the sill, where the overflow is still undiluted and not modified by entrained ambient water, are valuable to detect low-frequency variations and possible links to climate change signals.

[7] Here, we continue the time series introduced by Macrander *et al.* [2005], update the transport estimates and develop a method to fill some of the gaps in the time series where data from only one instrument exist. We discuss the variability on the different time scales (short term fluctuations to interannual variability and trends). Additionally, we present data from moored temperature and conductivity recorders, discuss the fluctuations in the hydrographic data and finally derive heat and salt flux contributions of the Denmark Strait overflow.

## 2. Data and Methods

### 2.1. Mooring Design

[8] The two moorings at the sill of Denmark Strait each consist of an ADCP in a floatation buoy, a SeaBird MicroCAT SBE-37SM (recording temperature, conductivity and pressure) and an IXSEA OCEANO release. The mooring positions are indicated in Figures 1 and 2. Mooring DS 1 ( $66^{\circ}4.6'N$ ,  $27^{\circ}5.6'W$ ) is at 650 m depth, while mooring DS 2 ( $66^{\circ}7.2'N$ ,  $27^{\circ}16.2'W$ ) is at 570 m depth. The instruments are placed close to the bottom, the release is only 6 m above the anchor. Directly attached to each release is a MicroCAT, followed by an ADCP buoy. The first bin measured by each ADCP is therefore only 26 m above the sea floor. The range of the instruments is approx. 600 m or 350 m, depending on the frequency of the ADCP and on environmental conditions like the amount of backscatter particles in the water column. The instrument at DS 1 was always a 75 kHz Longranger ADCP, while at DS 2 75 kHz Longranger and 150 kHz Quartermaster instruments were operated. A bin size of 16 m was chosen, as well as a sampling interval of 20 minutes; three measurements were combined to hourly ensembles with reduced errors. Tidal signals were removed from the velocity time series using T\_TIDE [Pawlowicz *et al.*, 2002], which provides a harmonic analysis of a time series and computes the tidal constituents. The MicroCAT sensors take a measurement every 10–20 minutes, depending on deployment, and daily averages were calculated, to get a temporal resolution similar to the transport time series (see below) and to reduce errors.

### 2.2. Transport Calculations

[9] After removal of the tides daily transport values were calculated, using the method of Macrander *et al.* [2005] based on results from high-resolution model simulations, extending

their time series in a consistent manner. The transport calculation uses the depth of maximum current shear as the upper boundary of the overflow layer. The resulting overflow layer thickness is on average 310 m at DS 1 and 280 m at DS 2. The measured velocities are rotated in the direction of the strait and the southwestward component is taken as the overflow leaving the Nordic Seas. Measurements from DS 1 are then considered to represent the flow over a width of 12.4 km, while DS 2 is used along a distance of 21.9 km. The unresolved flow on the Greenland shelf is approximated by adding another +0.4 Sv to the estimate [Macrander, 2004].

### 2.3. Filling Gaps in the Time Series

[10] Macrander *et al.* [2005] found that current profiles from two ADCPs are needed to calculate the overflow transports, which is in agreement with Käse and Oeschlies [2000], who reported single observations in Denmark Strait to be strongly contaminated by lateral variability and mesoscale eddies. Therefore, periods with data from only one instrument were not used for transport calculations in the past. By now the observations with two ADCPs add up to a time series of approximately eight years. While single current observations of one ADCP are biased by eddies, the conjunction of all the data is sufficient to reveal a significant dependence of the total transport on measurements obtained at DS 1. We introduce a linear model, based on the information of these eight years of data, to calculate overflow transports from the data of DS 1 alone. The regression of transport estimates of data from both ADCPs and from the ADCP at DS 1 only is shown in Figure 3. The regression was performed for the daily data as well as for 20 day low pass filtered transports. Both regressions show a significant correlation ( $r = 0.63$  and  $r = 0.55$ ). The standard error of the estimate is 1.26 Sv and 0.53 Sv, for daily and 20-day low pass filtered transports, respectively. The model based on the daily data was used to fill gaps in the transport time series, as it gave the better correlation. The derived model for the transport calculation thus reproduces 40% of the variance on a daily time scale.

### 2.4. Transport Uncertainties

[11] The instrumental error amounts to  $\pm 0.8 \text{ cm s}^{-1}$  per ensemble, with a compass error of  $\pm 5^{\circ}$ . The error in the overflow layer thickness from the maximum current shear is  $\pm 15 \text{ m}$ . Only on very few occasions the layer thickness was larger than the range of the 150 kHz Quartermaster ADCP; and the error on these occasions is higher. These instrumental errors add up to an error of  $\pm 0.15 \text{ Sv}$  for the transport estimates. The setup of the mooring array induces errors from passing eddies, which are not fully resolved. Derived from the model, Macrander [2004] determined this error to be up to 0.93 Sv for individual time steps. When considering time scales longer than the eddy scale (1–10 days) this error will get small (about 0.1 Sv). The assumptions made for the Greenland shelf transport are then one of the main uncertainties in the transport calculations, both due to the lack of mooring data and due to the uncertainty of the fate of the shelf waters, as they may feed into the East Greenland Spill Jet and not contribute to the overflow plume (see section 1). From observations, only vessel mounted ADCP data is available to validate the +0.4 Sv offset introduced from the model analysis (see above). The data does not contradict the

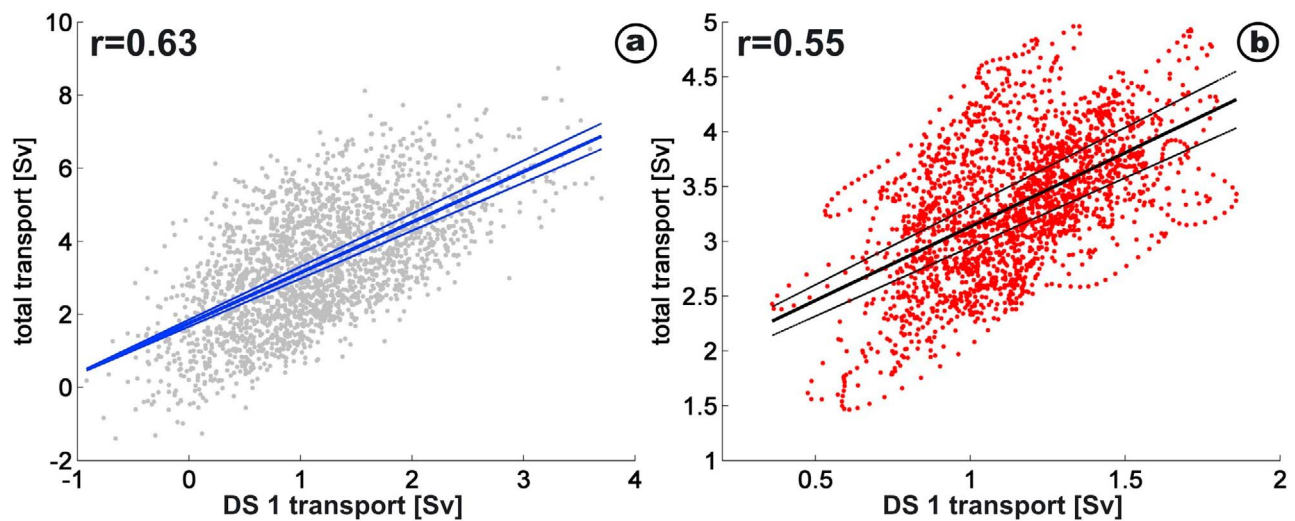


**Figure 3.** Regression of transport estimates from the DS 1 ADCP with transports estimates of both ADCPs (total transport), with 95% confidence intervals. (a) Daily data and (b) 20-day low pass filtered data. Note the different scales.

model results, but is too sparse to allow an independent estimate. The linear model based on the DS 1 ADCP developed to fill gaps in the transport time series underestimates the actual variability of the transport. The variance of the daily transport measured by two ADCPs is  $2.6 \text{ Sv}^2$ , while the variance of the daily transports in the model is only  $1.0 \text{ Sv}^2$ . Hence, the eddy variance of  $1.5 \text{ Sv}^2$  is missing in the reconstructed transports. The total mean transport is predicted accurately by the model.

## 2.5. Hydrographic Measurements

[12] The ADCPs also provide temperature measurements from a built-in sensor, with a precision of  $\pm 0.4^\circ\text{C}$ . The in-situ temperatures recorded by the ADCPs were highly correlated with the temperatures recorded by the MicroCATs ( $r > 0.95$ ), but exhibited offsets to the MicroCAT records. Therefore, the ADCP temperature records were only used to calculate the seasonal cycle, as longer time series exist from these sensors. Using the temperature data presented in *Macranders et al.* [2005], updated with the newer records, the seasonal cycle was obtained from a 13-year time series (starting in 1996, with gaps between deployments) at mooring DS 1. The MicroCATs were only recently added to the mooring deployments, starting in 2005. The MicroCAT temperature and salinity time series also contain gaps. The conductivity sensor at DS 1 recorded unrealistic data in 2007–2008, therefore the data was not used in this study.

## 3. Results

### 3.1. Transport Time Series

[13] The transport time series derived from the two moorings DS 1 and DS 2 is presented in Figure 4a, updated from *Macranders et al.* [2005] and *Quadfasel and Käse* [2007]. Gaps in the time series were filled using the linear model described above (see Data and Methods). In the following the transport will be discussed using the complete time series, with no distinction between the ‘two ADCP’ and ‘one ADCP’ transports (blue and magenta in the figure). The mean

transport for all deployment days (4337 days) is  $3.4 \text{ Sv}$  with a standard deviation of  $\pm 1.4 \text{ Sv}$ . The time series of the daily data demonstrates that the overflow in Denmark Strait exhibits energetic variability on many time scales, which is reflected in the high standard deviation (or the variance of  $2 \text{ Sv}^2$ ). The autocorrelation of the daily transport time series shows that transport estimates are independent after 5 days. To filter out the synoptic scale variability induced by eddies, which induce a variance of  $1.5 \text{ Sv}^2$  (see *Macranders et al.* [2007] for monthly spectra of the overflow transport), a 20-day low pass Hamming filter was applied (thick line in Figure 4a). The standard deviation of the filtered time series is only  $\pm 0.6 \text{ Sv}$ , which is nevertheless still about 20% of the mean transport.

[14] Hence, the present time series now allows a more precise estimate of the mean flow: the standard error of the mean (calculated from the standard deviation and the degrees of freedom of the time series, obtained by the autocorrelation) is only  $\pm 0.05 \text{ Sv}$ . Comparing this estimate to the previously calculated overflow in *Macranders et al.* [2005], which was  $3.5 \text{ Sv}$  for their 4-year time series (standard deviation  $\pm 1.6 \text{ Sv}$ ; standard error of  $\pm 0.14 \text{ Sv}$ ), the error of the mean is now reduced, but may still be biased by aliasing longer term variability not yet resolved. The low standard error indicates a high quality of the mean transport estimate due to the large amount of independent calculations. The total error of the mean, taking instrumental, random and statistical errors into account (cf. section 2), adds up to  $0.2 \text{ Sv}$  for the two-mooring array and  $1.3 \text{ Sv}$  for the one-mooring case. Uncertainties in the assumptions of the method are unknown and not taken into account here.

[15] On a daily resolution transports vary between  $-1.4 \text{ Sv}$  northeastward and  $8.7 \text{ Sv}$  southwestward. The high variability of the daily data is obvious for all deployment periods (Figure 4a). The day-to-day change of the overflow transport is typically of the order  $0.5 \text{ Sv}$ , but extreme changes of up to  $\pm 5.5 \text{ Sv}$  between one day to the next do occur. Nevertheless, the daily transport estimates show a nearly



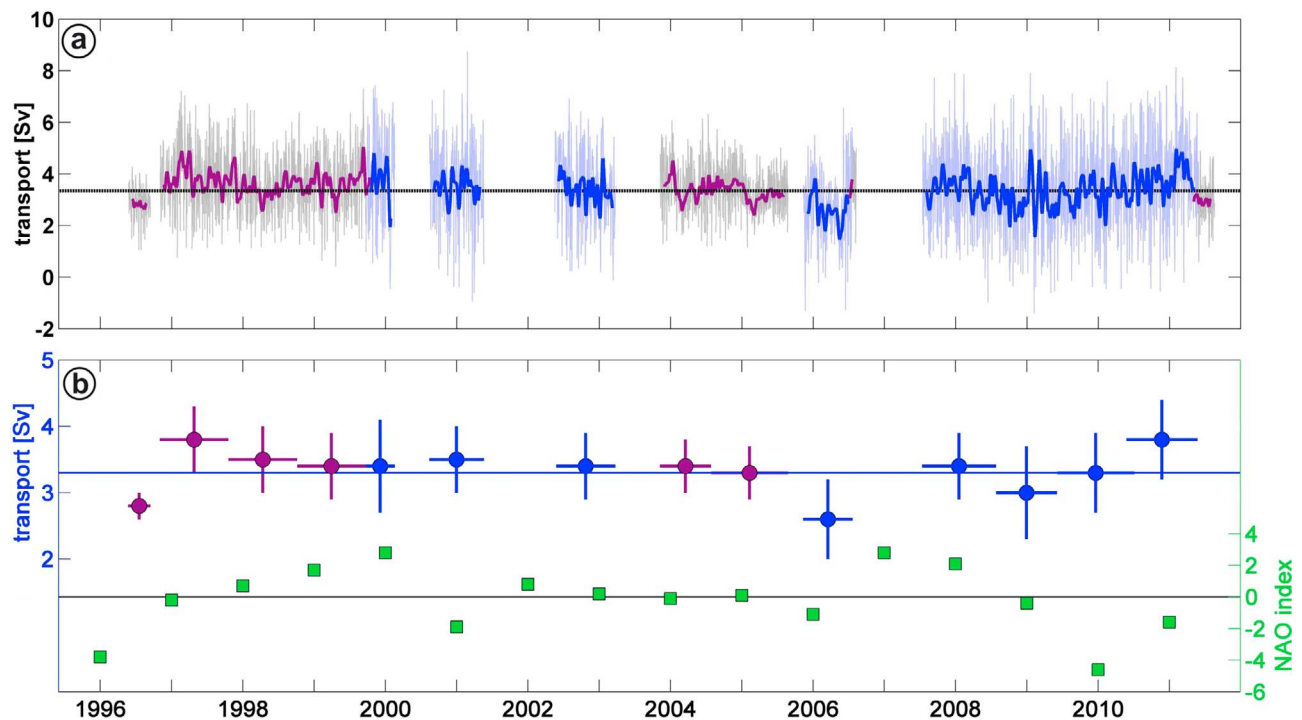


**Figure 4.** (a) Denmark Strait overflow transports in Sv. The 20-day low pass filtered transport derived from the moorings is depicted in blue, while the constructed transport from the linear model using data from DS 1 only is shown in magenta. Daily transports are illustrated in light blue and light grey in the background, respectively. The mean of the total time series is indicated by the dotted line. (b) Mean overflow transports for each deployment period (horizontal lines), with standard deviation (vertical lines) of the 20-day low pass filtered time series (according to Figure 4a). Additionally, the NAO winter index (Dec-Mar) is shown in green. (NAO Index Data provided by the Climate Analysis Section, NCAR, Boulder, USA, following Hurrell [1995]).

Gaussian distribution with a maximum around the mean of 3.4 Sv (a histogram is available in auxiliary material Figure S1).<sup>1</sup>

[16] The transport time series exhibits no pronounced seasonal modulation. Harmonic fits were applied to the two multi-year periods of the time series without gaps: 1997–2000 and 2007–2011. The resulting amplitudes are below 0.2 Sv in both cases and explain less than 5% of the variance. Calculating the monthly mean transports for all months in the time series illustrates the huge spread of the monthly data (Figure 5): the single estimates for each month vary within a 1–2 Sv range. Nevertheless, there are indications for a transport reduction in spring/summer and stronger transports in fall/winter, although the magnitude is very small (less than 10% of the total transport).

[17] From the variability of the annual mean transports of the deployment periods (Figure 4b) the interannual variability is determined to be typically on the order of  $\pm 0.3$  Sv. The low transport at the beginning of the time series (which is followed by a strong transport in the next deployment) is an exception, and may be due to the short duration of this mooring period producing a biased mean. The change between two successive estimates is below 1 Sv for all other deployments. The years 1999–2003 of the transport time series were presented in Macrandar *et al.* [2005], where the

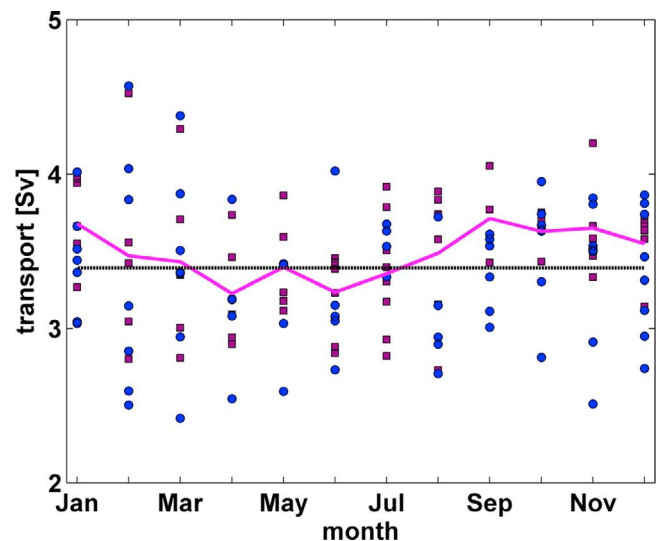


**Figure 5.** Monthly mean transports for all deployment periods (blue circles: data from two ADCPs, magenta squares: data from the DS 1 ADCP and the linear model). The black dotted line marks the mean transport, while the thick magenta line shows the total monthly mean.

<sup>1</sup>Auxiliary materials are available in the HMTL. doi:10.1029/2012JC008244.

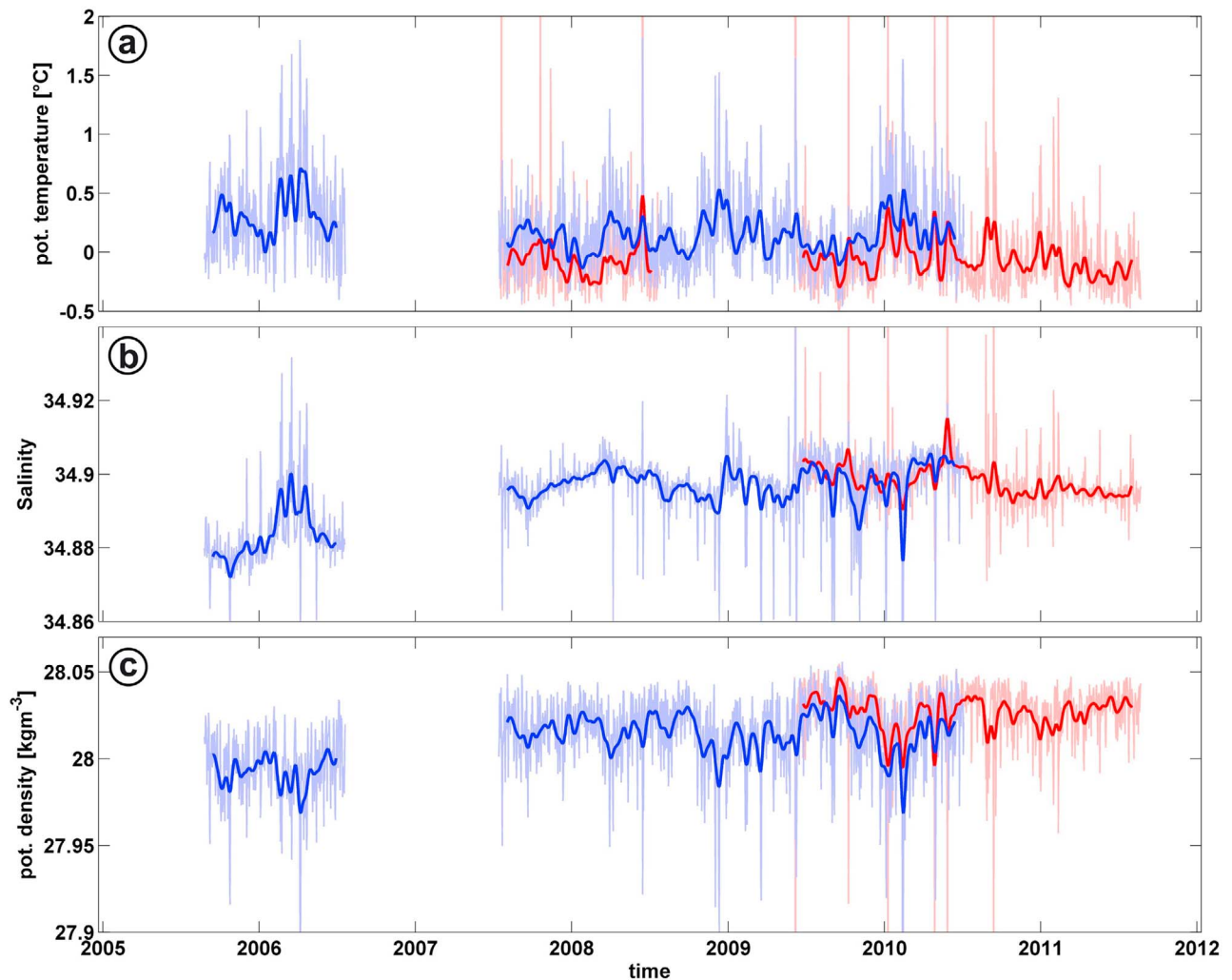


**Figure 6.** Hydrographic properties of the overflow close to the bottom of Denmark Strait, derived from the mooring records at DS 1 (red) and DS 2 (blue). (a) Potential temperature [°C]; (b) salinity; and (c) potential density anomaly  $\sigma_\theta$  [ $\text{kg m}^{-3}$ ]. Daily data are illustrated in light red/blue in the background, 20-day low pass filtered properties are depicted as thick lines.

authors reported a significant decrease of the overflow transport. The extended time series now shows, that the decrease persisted even during the next mooring period in 2005–2006. Nevertheless, after these low transports the new records from 2007–2011 revealed a recovery of the overflow; it was close to the mean and stronger in the last deployment period in 2010–2011 (3.8 Sv). The reason for strong/weak transport years is still unclear, a connection to e.g. the NAO winter index is not obvious (cf. Figure 4b). Overflow transports above the mean sometimes coincide with positive NAO winter indices, while weaker transports always correspond to negative indices; but a negative NAO index does not necessarily induce low overflow transports. The magnitude of the NAO signal seems to be of no importance. More data is needed to verify, if the overflow transport is linked to the NAO (suggested in *Blastoch et al.* [2003] through changing wind forcing), and to understand underlying processes. Connecting the overflow to local processes, as the wind stress curl over the strait, gives similarly ambiguous results: the maximum correlation found was below 0.4.

[18] In total, there is a weakening trend in the time series of  $-0.4$  Sv in 15 years, which explains 4% of the variance. Nevertheless, the trend is below the 70% confidence level of a Student's *t*-test and therefore not significant, and again, more data is needed to verify if the trend is persistent.

### 3.2. Hydrographic Time Series From MicroCAT Data

[19] High precision temperature, conductivity and pressure measurements were initiated in 2005. The recorded time series are presented in Figure 6, with daily averages in light colors in the background and 20-day low pass filtered time series as thick lines. The same filter as for the transport time series was used. The records from both instruments (at DS 1 and DS 2) show a similar variance, and are correlated on timescales longer than a few days ( $r > 0.6$  for the 20 day low pass filtered data). Therefore the shorter record of DS 1 was plotted in the background (red) in Figure 6, rather than in a separate figure.

[20] The mean hydrographic properties of the overflow with standard deviations of the 20-day low pass filtered time

**Table 1.** Mean Potential Temperature, Salinity and Potential Density Anomaly for the Mooring Records, With Standard Deviation<sup>a</sup>

	Mooring Period				
	2005–2006	2007–2008	2008–2009	2009–2010	2010–2011
<i>DS1</i>					
Mean $\theta$ (°C)	no data	−0.032	no data	−0.080	−0.095
Median $\theta$ (°C)	no data	−0.107	no data	−0.145	−0.168
Std $\theta$ (°C)	no data	±0.47	no data	±0.40	±0.32
Mean S	no data	no data	no data	34.901	34.896
Std S	no data	no data	no data	±0.029	±0.007
Mean $\sigma_\theta$ (kg m <sup>−3</sup> )	no data	no data	no data	28.026	28.027
Std $\sigma_\theta$ (kg m <sup>−3</sup> )	no data	no data	no data	±0.029	±0.018
Mean p (dbar)	no data	660	no data	653	659
<i>DS2</i>					
Mean $\theta$ (°C)	0.281	0.105	0.141	0.131	no data
Median $\theta$ (°C)	0.241	0.089	0.089	0.081	no data
Std $\theta$ (°C)	±0.37	±0.27	±0.31	±0.33	no data
Mean S	34.883	34.900	34.895	34.900	no data
Std S	±0.010	±0.006	±0.008	±0.013	no data
Mean $\sigma_\theta$ (kg m <sup>−3</sup> )	28.000	28.018	28.013	28.017	no data
Std $\sigma_\theta$ (kg m <sup>−3</sup> )	±0.020	±0.017	±0.021	±0.026	no data
Mean p (dbar)	557	574	571	565	no data

<sup>a</sup>For the potential temperature records, the median is given as well.

series (derived from the longer time series at DS 2, which has 1416 measurements; see Table 1 for mean properties at DS 1) are  $0.18^\circ\text{C} \pm 0.16^\circ\text{C}$  in potential temperature and  $34.894 \pm 0.008$  in salinity measured at 557–574 m depth, resulting in a mean density anomaly of  $28.01 \text{ kg m}^{-3} \pm 0.02 \text{ kg m}^{-3}$ . Autocorrelations of the hydrographic properties give a time-scale of decorrelation of 6 days. The respective standard errors are thus  $\pm 0.02^\circ\text{C}$ ,  $\pm 0.0006$  and  $\pm 0.002 \text{ kg m}^{-3}$ .

[21] The variability of the potential temperature on a daily resolution was typically in the order of  $0.1^\circ\text{C}$ . Overall, the potential temperature of the overflow at both moorings varied between  $-0.5^\circ\text{C}$  and  $1^\circ\text{C}$  (97% of all measurements), but occasionally warm events of up to  $5.1^\circ\text{C}$  (out of scale in Figure 6a) occurred (a histogram of the temperature data is available in auxiliary material Figure S2). These warm events only lasted for a few hours to two days, and they were more frequent at mooring DS 1 (and with higher amplitude) than at mooring DS 2. 26 anomalies exceeding  $2^\circ\text{C}$  were noted at DS 1, at irregular intervals (the mean time step between events is 46 days). Similar anomalies are present in the salinity time series, which showed less variance on a daily basis (typical day-to-day change of 0.001), as seen in Figure 6b.

[22] The time series of the potential density anomaly  $\sigma_\theta$  (Figure 6c) reveal that all warm events result in lower than normal densities. In both records the potential density anomaly never exceeded  $28.056 \text{ kg m}^{-3}$ . Apparently, denser water was unable to pass the sill of Denmark Strait during our mooring period. The minimum potential density anomaly found at DS 1 was  $27.70 \text{ kg m}^{-3}$  and  $27.82 \text{ kg m}^{-3}$  at DS 2. Hence, all events noted at DS 2 are still in the density range of the overflow ( $>27.8 \text{ kg m}^{-3}$ ), but at DS 1 warmer, saltier waters influence the measurements, which cannot be attributed to the classically defined overflow. These waters correspond to the Atlantic inflow (warm and saline anomalies), which is normally found closer to the Icelandic shelf. Since mooring DS 1 is located closer to Iceland than mooring DS 2, intrusions of Atlantic water are more likely at this

position. The low salinity, low density anomalies found at DS 2 rather indicate variations in the composition of the overflow (e.g. a higher influence of East Greenland Current waters).

[23] The seasonal cycle of the potential temperature was obtained from the temperature sensors at the ADCPs (see Data and Methods), as these records are much longer than the period of the MicroCAT measurements. High temperatures occur during March, while the minimum temperature in the seasonal cycle was found in September. Although the seasonal variability is rather small (the amplitude of the seasonal cycle is only  $0.09^\circ\text{C}$ ) it is nevertheless statistically significant, and corresponds to the seasonal analysis of downstream temperature data by *van Aken and de Jong* [2012] near Cape Farewell. Similar small amplitudes are found for salinity and density from the MicroCAT record at DS 2: the amplitude in salinity is  $0.003$  with maxima in April and minima in October, and  $0.007 \text{ kg m}^{-3}$  for density with maxima in August and minima in February. Seasonal variability explains less than 5% of the variance in the hydrographic time series and shows different phases when computed for the different instruments/deployment periods.

[24] The deployment mean hydrographic properties are presented in Table 1; only the temperature data was de-seasoned, since it is based on a time series covering many seasonal periods (which is not the case yet for salinity). To reduce the influence of warm and cold events at the mooring positions, the median was calculated for the potential temperature data as well as the mean. The median is always colder than the mean, as expected. Additionally the potential temperatures at DS 1 are lower than at DS 2, which is a result of the deeper location of the mooring. The variation of potential temperature and salinity at mooring DS 2 indicate interannual variability of the potential density anomaly in the range of  $\pm 0.004$ – $0.018 \text{ kg m}^{-3}$ .

[25] The deployment potential temperatures in Table 1 thus indicate a cooling of the overflow from 2005–2006 to

2007–2008 at DS 2. The changes since 2008 are within the range of the error and therefore not significant. A cooling of the overflow was evident at DS 1 as well, between 2007–2008 and 2009–2010. Whether the observed cooling represents interannual variability or a long term trend remains an open question, and can only be solved when the time series is longer. Nevertheless, the warming trend reported in *Macrander et al.* [2005] is not confirmed from our MicroCAT observations. For salinity, the records indicate an increase from 2005–2006 to 2007–2008. After that, the salinity stayed nearly constant. All changes are close to the accuracy of the measurements.

### 3.3. Heat and Salt Transports

[26] Although our measurements focus only on one exchange process through the Greenland Scotland Ridge, our results can be used to improve estimates of heat and salt fluxes across the Ridge as presented by *Østerhus et al.* [2005] and more recently by *Rosby and Flagg* [2012]. The overflow contribution to the total meridional heat flux (OHF) is derived by combining the transport estimates ( $v$ ) with the temperature data ( $T$ ), multiplying with the heat capacity of sea water ( $c_p$ ) and the mean density ( $\rho$ ):  $OHF = v \cdot T \cdot c_p \cdot \rho$ . The flux is subdivided into the eddy heat flux and the mean heat flux, obtained by using either the temperature flux fluctuations  $\langle v'T' \rangle$  or the mean  $\langle v\bar{T} \rangle$ . The overflow thus exhibits an eddy heat flux of 2.1 TW (1 TW =  $10^{12}$  W) and the mean heat flux referenced to 0°C is 2.8 TW. Combining the eddy heat flux and the mean temperature flux, the heat flux contribution of the Denmark Strait overflow is hence in the order of 5 TW. Assuming an uncertainty of the transport calculation of 1 Sv (which certainly induces the largest error), results in an error of  $\pm 0.8$  TW for the heat flux. When calculating the budget of the Nordic Seas, the contribution of the Denmark Strait overflow is rather small and can be neglected (total Atlantic inflow: 313 TW, *Østerhus et al.* [2005]). Considering the heat exchanges through Denmark Strait only, which exhibits 24 TW of Atlantic inflow in the IC [*Jónsson and Valdimarsson*, 2012; *Østerhus et al.*, 2005], the overflow amounts to about 20% of this inflow and has to be considered.

[27] Our heat flux estimate strongly depends on the temperatures  $\bar{T}$  and  $T'$ ; and since we only have near bottom measurements, the derived heat flux contribution can only be taken as a rough estimate. Profiles taken at the mooring position indicate that the bottom temperature is representative of an approx. 100 m thick layer. Our approximation using the bottom temperature is supported by *Dickson et al.* [2008], who described the overflow as temperature stratified in the upper part, but homogeneously cold in the lower layer, which represents the largest fraction of the plume.

[28] The salt flux contribution is obtained by weighting the overflow volume flux with the average salinity (referenced to  $S = 0$ ). The salt flux derived from this method is  $119 \text{ kT s}^{-1}$  ( $\text{kT s}^{-1} = 10^6 \text{ kg s}^{-1}$ ). Assuming again an uncertainty of the transport calculation of 1 Sv leads to an error of  $\pm 35 \text{ kT s}^{-1}$  for the salt flux estimate. Compared to the Atlantic inflows analyzed in *Østerhus et al.* [2005], the overflow is not negligible. Due to the weak volume transport of 0.88 Sv, the salt flux of the Atlantic inflow branch in Denmark Strait is only  $30 \text{ kT s}^{-1}$ . The stronger Faroe and Shetland branches contribute  $133 \text{ kT s}^{-1}$  and  $139 \text{ kT s}^{-1}$  to the northward salt flux

[*Østerhus et al.*, 2005]. Hence, the overflow contributes significantly to the salt (or freshwater) budget of the Nordic Seas.

## 4. Discussion

[29] The mooring data of the Denmark Strait overflow reveals the stability of the supply of water flowing from the Nordic Seas into the Atlantic, which agrees well with downstream measurements of the Deep Western Boundary Current (DWBC) [*Fischer et al.*, 2010]. Nevertheless, variability on all time scales occurs and many open questions regarding the relevant processes remain. To detect possible climate signals, and to verify modeling results, it is essential to extend the time series and understand the causes of the variability. When only a few years of data are analyzed, interannual variability can be misinterpreted as long term trends. While the data allow a statistically precise estimate of the mean transport, long time series (several decades of data) of observations are needed to detect climate trends with confidence, as e.g. a study of *Baehr et al.* [2006] has shown. Similar to the results from the Faroe Bank Channel overflow [*Hansen and Østerhus*, 2007], no significant long term trend is identified in the time series from the Denmark Strait overflow. The overflows are expected to decrease in transport in a future warming climate, since a reduction of the Atlantic Overturning Circulation will likely be imprinted on the overflow transports, but whether this weakening is already happening cannot be determined with confidence from the current data.

[30] The transport time series exhibit no distinct seasonal modulation, as harmonic fits for the two continuous multi-year periods showed (1997–2000 versus 2007–2011). The hydrographic time series confirm the minor importance of the seasonal frequency for the Denmark Strait overflow at the sill: all seasonal cycles for the available parameters (transport as well as pot. temperature, salinity and density) explain less than 5% of the variance in the time series. The results on the seasonal cycle and the warm events found in the Denmark Strait overflow differ from those reported for the Faroe Bank Channel overflow [*Hansen and Østerhus*, 2007], which is constantly cold (temperatures ranging between 0.1 and  $-0.8^\circ\text{C}$ ); no outstanding warm events occurred. The bottom temperature in the Faroe Bank Channel, as well as the transport, exhibits a clear seasonality.

[31] The lack of a seasonal cycle in our observations is in conflict with modeling studies, which identified a seasonal transport variability of the Denmark Strait overflow featuring a maximum in late summer [*Köhl et al.*, 2007; *Köhl*, 2010]. The total transport through Denmark Strait in the *Köhl et al.* [2007] model is only 2.5 Sv (thus 25% lower than the observational estimate), and their seasonal cycle is about one fourth of the total transport. This discrepancy between the observed seasonal variability and modeled transports was already noted in *Bjastoch et al.* [2003], so the discrepancy is still valid for modern, high resolution models. The issue should be addressed in the future, since it may reveal important differences in the forcing mechanisms between the model and the real ocean.

[32] Downstream of Denmark Strait the overflow gains volume by entrainment, and becomes one of the main



contributors to the DWBC. Measurements along the pathway of the overflow confirm the absence of seasonality [Hall *et al.*, 2011; Fischer *et al.*, 2010], and show a dampening of the high frequency variability. Near Ammassalik variability on the eddy scale of 3–10 days is still noted [Voet and Quadfasel, 2010; Hall *et al.*, 2011], while in the DWBC in the Labrador Sea the high frequency variability is on the scale of weeks with reduced energy [Fischer *et al.*, 2010]. Interannual variability was found to be approx. 10% of the mean in the DBWC, which is remarkably similar to our results of the overflow at the sill.

[33] Power spectra of the transport and the hydrographic properties from Denmark Strait (not shown) both depict high energy in the 2–10 days period band; and high frequency variability was noted in all daily time series, but the actual correlation between the transport and the pot. temperature or salinity is low (on all time scales:  $r < 0.3$ ). The low correlation between salinity anomalies and overflow transport was already noted further downstream of the sill at Ammassalik [Hall *et al.*, 2011], as well as near Cape Farewell [van Aken and de Jong, 2012], and interpreted as consequences of changes in the source water contributions. Sudden shifts in the overflow temperature, similar to the temperature record from DS 2, were also noted by Macrander *et al.* [2007]. The authors attributed these shifts to changes in the relative contributions of the source water masses of the overflow, rather than to changing properties of the sources. This interpretation is in agreement with the findings of Köhl [2010], where a high resolution ocean model was used to analyze the different sources of the Denmark Strait overflow waters for varying wind forcing. While the time series presented here confirm the variability, a link to varying wind forcing/NAO (which was also proposed in Serra *et al.* [2010]) could not be established. The approach of Våge *et al.* [2011] sorts the temperature measurements into “Atlantic” ( $\theta > 0^\circ\text{C}$ ) and “Arctic” ( $\theta < 0^\circ\text{C}$ ) source water classes. Applying this method to our data shows the dominance of the “Arctic” sources in the deep overflow: most measurements from DS 1 (70% of the daily temperatures) are below the threshold of  $0^\circ\text{C}$  (cf. auxiliary material Figure S2), while at DS 2 the Atlantic sources dominate (only 30% of the temperatures are  $< 0^\circ\text{C}$ ). This result is in agreement with Våge *et al.* [2011], who found mostly Arctic waters at the deepest part of the Denmark Strait sill. The maximum potential density anomaly observed at the moorings was  $28.056 \text{ kg m}^{-3}$ . Østerhus *et al.* [2005] showed that this water is a mixture of upper Polar Deep Water, Greenland Sea Arctic Intermediate Water and Iceland Sea Arctic Intermediate Water, which is probably transported to Denmark Strait within the North Icelandic Jet.

[34] Meandering of the Irminger Current influences the mooring at the deepest position of the sill of Denmark Strait (DS 1). Warm events related to the Atlantic Water inflow into the Nordic Seas occurred at irregular intervals. The extreme warm events always coincided with lower than average transports. In Jónsson and Valdimarsson [2005] mooring results from the shelf area north of Iceland were discussed. The authors point out that the warm and saline Atlantic inflow waters are confined to the upper 200 m. From our mooring results, we note that the Atlantic inflow at times reaches the bottom of Denmark Strait, which is 640 m. The induced warm events in the near bottom layer apparently do not reach the latitude of the Jónsson and

Valdimarsson [2005] study region and must take another path or recirculate. The fate of this deep flow of Atlantic water is so far unknown.

[35] The mean temperature and salinity records for the different mooring periods indicate a cooling and slightly increasing salinity in the near-bottom overflow. The rapid freshening trend of the overflow and the whole deep Atlantic Ocean described in Dickson *et al.* [2002] has stopped, and the salinity has increased again. The mean salinity of the 2005–2006 deployment period (Table 1) is in the range of the low salinities measured during 1993–2002, while the data since 2007 corresponds to the early 1990s and 1977 [cf. Dickson *et al.*, 2002, Figure 2]. An increase in salinity of the same magnitude was found in the Faroe Bank Channel as well [Hansen and Østerhus, 2007], which resulted in an increase in density of  $0.01 \text{ kg m}^{-3}$ , similar to our results at DS 2. Whether the observed salinity change indicates a reversal of the trend, or changes in the source water contributions, or interannual variability, must be answered in the future, when more data is available. The light and warm anomalies found in the Arctic [Karcher *et al.*, 2008] thus did not cause anomalously light overflow water in recent years. Especially the warm events described in Karcher *et al.* [2011] were not noticed in our overflow measurements so far, and the predicted 30% reduction of the transport has not occurred yet.

[36] The Denmark Strait overflow contribution to the meridional heat flux across the Greenland Scotland Ridge obtained by our mooring results is 5 TW and thus negligible for the budget of the Arctic Mediterranean. Our estimate is much smaller than the 27 TW given in Rossby and Flagg [2012], who used the mean overflow properties at Ammassalik. However, the overflow exhibits a rapid temperature increase as it descends into greater depth in the Irminger Sea downstream of the sill [Dickson *et al.*, 2008]; and using the lower temperatures directly at the sill is thus more accurate. Rossby and Flagg [2012] give a residual southward salt export through Denmark Strait of  $1.45 \cdot 10^8 \text{ kg s}^{-1}$ , which was obtained by the budget of all other fluxes, assuming steady state conditions. Considering our salt flux estimates from measurements taken directly at the sill ( $1.19 \cdot 10^8 \text{ kg s}^{-1}$ , using the same units as Rossby and Flagg [2012]) leaves an unresolved flux of  $0.3 \cdot 10^8 \text{ kg s}^{-1}$ , which may be attributed to the East Greenland Current.

[37] **Acknowledgments.** We acknowledge the contributions of the captains and crews of the research vessels R/V *Meteor*, R/V *Maria S. Merian*, R/V *Knorr*, R/V *Arni Fridriksson* and R/V *Bjarni Saemundsson* in the mooring work. We thank Andreas Macrander for providing Matlab routines for quality control and transport calculations. We also thank Rolf Käse for helpful discussions and comments on the interpretation of the time series. This work was funded by the German Federal Ministry for Education and Research (BMBF), Förderkennzeichen 03F0605A (AP 2.3), and by the European Commission in the project THOR, grant agreement 212643. A grant from the Icelandic Centre for Research is also acknowledged. Finally we thank two anonymous reviewers, who helped to improve the quality of the manuscript.

## References

- Baehr, J., K. Keller, and J. Marotzke (2006), Detecting potential changes in the meridional overturning circulation at  $26^\circ\text{N}$  in the Atlantic, *Clim. Change*, 20, 145–157, doi:10.1007/S10584-006-9153-Z.
- Biaosch, A., R. Käse, and D. Stammer (2003), The sensitivity of the Greenland-Scotland Ridge overflow to forcing changes, *J. Phys. Oceanogr.*, 33, 2307–2319.

- Breareley, J., R. Pickart, H. Valdimarsson, S. Jonsson, R. Schmitt, and T. Haine (2012), The East Greenland boundary current system south of Denmark Strait, *Deep Sea Res., Part I*, 63, 1–19.
- Dickson, B., I. Yashayaev, J. Meincke, B. Turrell, S. Dye, and J. Holfort (2002), Rapid freshening of the deep North Atlantic Ocean over the past four decades, *Nature*, 416, 832–837.
- Dickson, B., et al. (2008), The overflow flux west of Iceland: Variability, origins and forcing, in *Arctic-Subarctic Ocean Fluxes*, edited by R. R. Dickson, J. Meincke, and P. Rhines, pp. 443–474, Springer, New York.
- Dickson, R., and J. Brown (1994), The production of North Atlantic Deep Water: Sources, rates, and pathways, *J. Geophys. Res.*, 99(C6), 12,319–12,341.
- Falina, A., A. Sarafanov, H. Mercier, P. Lherminier, A. Sokov, and N. Danialt (2012), On the cascading of dense shelf waters in the Irminger Sea, *J. Phys. Oceanogr.*, doi:10.1175/JPO-D-12-012.1, in press.
- Fischer, J., M. Visbeck, R. Zantopp, and N. Nunes (2010), Interannual to decadal variability of outflow from the Labrador Sea, *Geophys. Res. Lett.*, 37, L24610, doi:10.1029/2010GL045321.
- Girton, J., T. Sanford, and R. Käse (2001), Synoptic sections of the Denmark Strait overflow, *Geophys. Res. Lett.*, 28(8), 1619–1622.
- Hall, S., S. Dye, K. Heywood, and M. Wadley (2011), Wind forcing of salinity anomalies in the Denmark Strait overflow, *Ocean Sci. Discuss.*, 8, 1403–1440, doi:10.5194/osd-8-1403-2011.
- Hansen, B., and S. Østerhus (2007), Faroe Bank Channel overflow 1995–2005, *Prog. Oceanogr.*, 75, 817–856, doi:10.1016/j.pocan.2007.09.004.
- Hurrell, J. W. (1995), Decadal trends in the North Atlantic Oscillation: Regional temperatures and precipitation, *Science*, 269, 676–679.
- Jónsson, S., and H. Valdimarsson (2005), The flow of Atlantic Water into the North Icelandic Shelf and its relation to the drift of cod larvae, *ICES J. Mar. Sci.*, 62, 1350–1359, doi:10.1016/j.icesjms.2005.05.003.
- Jónsson, S., and H. Valdimarsson (2012), Water mass transport variability to the North Icelandic shelf, 1994–2010, *ICES J. Mar. Sci.*, doi:10.1093/icesjms/fss024, in press.
- Karcher, M., R. Gerdes, and F. Kauker (2008), Long-term variability of Atlantic Water inflow to the northern seas: Insights from model experiments, in *Arctic-Subarctic Ocean Fluxes*, edited by R. R. Dickson, J. Meincke, and P. Rhines, pp. 111–129, Springer, New York.
- Karcher, M., A. Beszczynska-Möller, F. Kauker, R. Gerdes, S. Heyen, B. Rudels, and U. Schauer (2011), Arctic Ocean warming and its consequences for the Denmark Strait overflow, *J. Geophys. Res.*, 116, C02037, doi:10.1029/2010JC006265.
- Käse, R., and A. Oschlies (2000), Flow through Denmark Strait, *J. Geophys. Res.*, 105(C12), 28,527–28,546.
- Köhl, A. (2010), Variable source regions of Denmark Strait and Faroe Bank Channel overflow waters, *Tellus, Ser. A*, 62, 551–568, doi:10.1111/j.1600-0870.2010.00454.x.
- Köhl, A., R. Käse, D. Stammer, and N. Serra (2007), Causes of changes in the Denmark Strait overflow, *J. Phys. Oceanogr.*, 37, 1678–1696, doi:10.1175/JPO3080.1.
- Macrander, A. (2004), Variability and processes of the Denmark Strait overflow, dissertation, Univ. of Kiel, Kiel, Germany.
- Macrander, A., U. Send, H. Valdimarsson, S. Jónsson, and R. H. Käse (2005), Interannual changes in the overflow from the Nordic Seas into the Atlantic Ocean through Denmark Strait, *Geophys. Res. Lett.*, 32, L06606, doi:10.1029/2004GL021463.
- Macrander, A., R. H. Käse, U. Send, H. Valdimarsson, and S. Jónsson (2007), Spatial and temporal structure of the Denmark Strait overflow revealed by acoustic observations, *Ocean Dyn.*, 57, 75–89, doi:10.1007/s10236-007-0101-x.
- Olsson, K., E. Jeansson, T. Tanhua, and J. Gascard (2005), The East Greenland Current studied with CFCs and released sulphur hexafluoride, *J. Mar. Syst.*, 55, 77–95.
- Østerhus, S., W. Turrell, S. Jónsson, and B. Hansen (2005), Measured volume, heat and salt fluxes from the Atlantic to the Arctic Mediterranean, *Geophys. Res. Lett.*, 32, L07603, doi:10.1029/2004GL022188.
- Pawlowicz, R., B. Beardsley, and S. Lentz (2002), Classical tidal harmonic analysis including error estimates in MATLAB using T TIDE, *Comput. Geosci.*, 28, 929–937.
- Quadfasel, D., and R. Käse (2007), Present-day manifestation of the Nordic Seas overflows, in *Ocean Circulation: Mechanisms and Impacts*, *Geophys. Monogr. Ser.*, vol. 173, edited by A. Schmittner et al., pp. 75–90, AGU, Washington, D. C., doi:10.1029/173GM07.
- Ross, C. (1984), Temperature-salinity characteristics of the “overflow” water in Denmark Strait during “OVERFLOW 73,” *Rapp. P.-V. Reun. Comm. Int. Explor. Sci. Mer Mediterr.*, 185, 111–119.
- Rosby, T., and C. Flagg (2012), Direct measurement of volume flux in the Faroe-Shetland Channel and over the Iceland-Faroe Ridge, *Geophys. Res. Lett.*, 39, L07602, doi:10.1029/2012GL051269.
- Rudels, B., E. Fahrback, J. Meincke, G. Budéus, and P. Eriksson (2002), The East Greenland Current and its contribution to the Denmark Strait overflow, *ICES J. Mar. Sci.*, 59, 1133–1154, doi:10.1006/jmsc.2002.1284.
- Serra, N., R. Käse, A. Köhl, D. Stammer, and D. Quadfasel (2010), On the low-frequency phase relation between the Denmark Strait and the Faroe-Bank Channel overflows, *Tellus, Ser. A*, 62(4), 530–550, doi:10.1111/j.1600-0870.2010.00445.x.
- Tanhua, T., K. Olsson, and E. Jeansson (2005), Formation of Denmark Strait overflow water and its hydro-chemical composition, *J. Mar. Syst.*, 57, 264–288.
- Våge, K., R. Pickart, M. Spall, H. Valdimarsson, S. Jónsson, D. Torres, S. Østerhus, and T. Eldevik (2011), Significant role of the North Icelandic Jet in the formation of Denmark Strait overflow water, *Nat. Geosci.*, 4, 723–727, doi:10.1038/NGEO1234.
- van Aken, H., and M. de Jong (2012), Hydrographic variability of Denmark Strait overflow water near Cape Farewell with multi-decadal to weekly time scales, *Deep Sea Res., Part I*, 66, 41–50.
- Voet, G., and D. Quadfasel (2010), Entrainment in the Denmark Strait overflow plume by meso-scale eddies, *Ocean Sci. Discuss.*, 6, 301–310.
- Worthington, L. (1969), An attempt to measure the volume transport of Norwegian Sea overflow water through the Denmark Strait, *Deep Sea Res.*, 16, supplement, 421–432.